Transport and optical properties of holes in p-type zero-band-gap $Hg_{1-x}Zn_xTe/CdTe$ superlattices

J. B. Choi, K. H. Yoo,* J. W. Han,† and T. W. Kang‡
Department of Physics, Chungbuk National University, Cheongju, 360-763, Korea

J. R. Meyer and C. A. Hoffman
Naval Research Laboratory, Washington, D.C. 20375

G. Karczewski and J. K. Furdyna
Department of Physics, University of Notre Dame, Notre Dame, Indiana 47907

J. P. Faurie
Department of Physics, University of Illinois, Chicago, Illinois 60680
(Received 1 November 1993)

Transport, reflectivity, and magneto-optical measurements have been performed on a p-type zero-band-gap $Hg_xZn_{1-x}Te/CdTe$ superlattice for systematic investigation of the anomalous properties of holes. The observed magnetotransport, intrasubband, and intersubband optical-transition data are fully correlated with a $\mathbf{k}\cdot\mathbf{p}$ band calculation and show consistent behavior resulting from two holes with different mobilities. The distinctive features of the holes are accurately explained by the extremely nonparabolicity and anisotropic nature of the valence-band structure.

I. INTRODUCTION

Recent comprehensive theoretical treatments[1-3] of electronic properties of Hg-based superlattices have demonstrated that a number of peculiar band-edge properties may be attributed to unique features of narrow-gap superlattice band structures, which are quite distinct from anything observed so far in wide-gap systems. In particular, ultrahigh hole mobilities ($>10^5$ cm^2/V s), observed in zero-gap HgTe/CdTe superlattices,[4,5] are obtained from the extremely small in-plane hole effective masses and arise from the unique structure of the lowest-order heavy-hole valence band near the band edge. The existence of holes with such high mobilities is of great interest for devices, and their electronic and optical properties need to be further investigated related to the peculiar structure of the valence band. Here we report a systematic experimental investigation of the anomalous properties of holes in a p-type $Hg_{1-x}Zn_xTe/CdTe$ superlattice by performing reflectivity, transport, and magneto-optical measurements. $Hg_{1-x}Zn_xTe/CdTe$ superlattices are speculated to be better in stability than traditional HgTe/CdTe superlattices because of the presence of Zn. For example, whereas the transport and magneto-optical properties of HgTe/CdTe superlattices sometimes deteriorate considerably with time, the carrier concentrations and high hole mobilities in the present HgZnTe/CdTe superlattice were virtually unchanged after nearly five years. Early studies[6,7] on $He_{1-x}Zn_xTe/CdTe$ superlattices were confined to magneto-optical properties of electrons to resolve the controversial value of the valence-band offset by using conduction-band anisotropy. In our studies of the p-type zero-gap $Hg_{1-x}Zn_xTe$ superlattice, transport and cyclotron-resonance data are fully correlated with the polarization-dependent reflectivity, and show consistent behavior of the holes implied by the unique structure of the valence band. Considering the compensating effects of quantum confinement and strain on the positions of the hole subbands, this study also gives direct experimental evidence for a large value ($\simeq 500$ meV) of the valence-band offset.

II. EXPERIMENT

Transport, cyclotron-resonance, and reflectivity measurements have been performed on a 100-period p-type $Hg_{1-x}Zn_xTe/CdTe$ superlattice grown by molecular-beam epitaxy on a (100) GaAs substrate. Nominal material parameters are $x=0.06$ for the composition of the $Hg_{1-x}Zn_xTe$ wells, 70 Å for the well thickness, and 23 Å for the CdTe barrier thickness. However, these values will be adjusted slightly (within their experimental uncertainties) in the band-structure calculations discussed later, in order to assure consistency with the experimental finding that the superlattice is nearly semimetallic. Van der Pauw Hall and conductivity measurements were performed as a function of magnetic field up to 7 T and for temperatures down to 4.2 K. Free carrier densities and mobilities have been determined by performing a mixed conduction analysis. For the far-infrared transmission measurements, the sample was mounted in the Faraday geometry inside an optical cryostat at the center of a split-coil 6-T superconducting solenoidal magnet. An optically pumped cw laser provided far-infrared photon energies ranging from $\lambda=70.6$ to 496 μm. The radiation was circularly polarized using a linear polarizer followed by crystal quartz $\lambda/4$ plates. For the reflectivity measurements, we employed a

BOMEM Fourier transform infrared spectrometer for using higher excitation photon energies required to measure intersubband optical transitions, and developed a reflectivity technique to enhance the polarization perpendicular to the superlattice plane. The broadband beam was incident at 45° to the back side of the sample, i.e., the GaAs substrate. A conducting thin film was tightly attached to the front of the superlattice film. The presence of the conducting plate causes the optical electric field to be predominantly perpendicular to the superlattice plane, the polarization of which gives maximum optical coupling of the radiation to the vertical motion of electrons. A linear polarizer (KRS-5) was used to change the polarization of the incident beam.

III. TRANSPORT AND MAGNETOTRANSMISSION

Figures 1 and 2 show the temperature-dependent electron and hole concentration and mobility data obtained from the mixed conduction analysis in which two hole species and two electron species were required to obtain the best fit. Typical hole cyclotron-resonance data in Faraday geometry (optical propagation parallel to B) at 1.8 K are shown in Fig. 3 for three far-infrared photon energies $\hbar\omega$. Figures 4(a) and 4(b) display temperature dependence of hole and electron cyclotron resonances for a $\hbar\omega = 10.44$ meV in Faraday geometries, respectively. All the data show consistent behavior as follows. First, at low temperatures ($T < 10$ K) two hole species with different mobilities obtained from the mixed-conduction analysis of the magnetotransport data correspond to the two-hole cyclotron resonances observed in the hole-active circular polarization of Faraday geometry. The hole cyclotron mass associated with the lower field resonance is found to be $\simeq 2.5\times10^{-3}m_0$, which is extremely small and results in the ultrahigh hole mobility observed in transport. The second hole resonance corresponding to the lower mobility holes in transport is resolved only for high resonance magnetic fields because of its broader linewidth. With increasing temperature ($T > 110$ K) thermally generated intrinsic electrons come to dominate the transport properties, and they are also reflected in the cyclotron-resonance data: two electron cyclotron resonances start to occur, while the intensities of the hole absorptions decrease. This thermal behavior of carriers indicates that the sample has an energy gap near zero. The theoretical fit of magneto-optical transition data, which will be shown in the next section, yields a slight positive or negative band gap of magnitude of about 6 meV. However, since the electron concentration indicated by the transport data at 15 K should have been a factor of 5 lower than that measured if a positive gap as large as 6 meV was present, we conclude that this p-type sample is a semimetallic superlattice with a negative gap. The Fermi level at 0 K lies about 3 meV below the valence-band

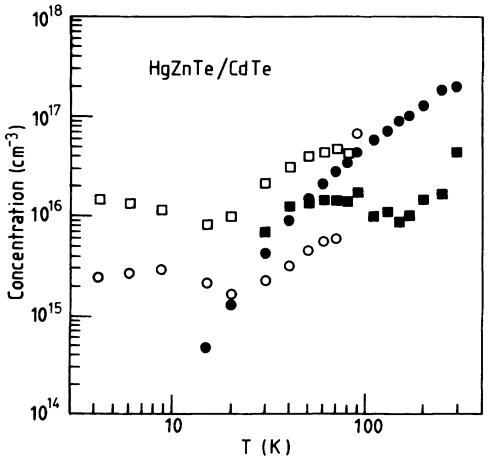

FIG. 1. Temperature dependence of electron and hole concentrations (holes, open marks: electrons, solid marks).

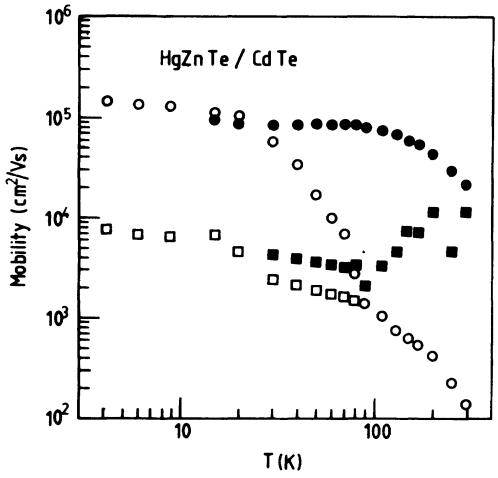

FIG. 2. Temperature dependence of electron and hole mobilities (holes, open marks; electrons, solid marks).

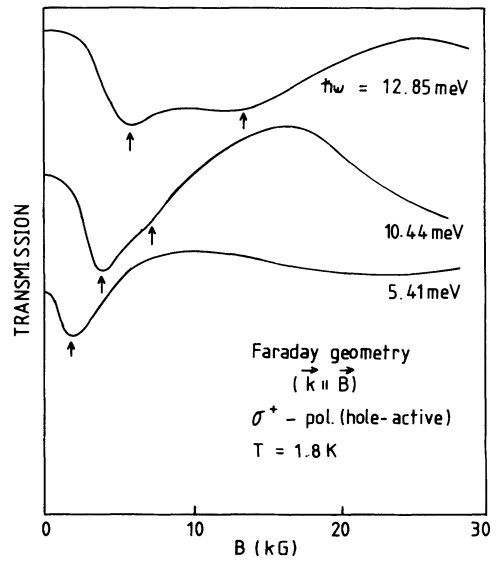

FIG. 3. Far-infrared photon energy dependence of cyclotron resonance for hole-active polarization in Faraday geometry at 1.8 K.

maximum and conduction-band minimum and we do not expect any electrons to be present in the zero-temperature limit.

Figure 5 shows compilations of the electron and hole cyclotron-resonance data in Faraday configuration. The solid curves are the calculated inter-Landau-level transition energies, which will be discussed in Sec. IV. Only the higher field electron resonance cannot be fit by any inter-Landau-level transitions of superlattices, but its broad linewidth and heavy effective mass accounts for the low mobility electron measured in transport. The transport data provide that whereas the mixed-conduction analysis yields only two-hole species in the low-temperature limit, the superlattice electron appears at 15 K and a second electron with lower mobility becomes resolvable at 30 K. This consistency between transport and cyclotron resonance suggests that the higher field electron resonance may be due to interface carriers between the superlattice and the CdTe buffer layer. The enhanced surface scattering and nonparabolicity may explain the lower mobility and heavy cyclotron effective mass associated with the high-field electron cyclotron resonance. However, we point out that the conclusive identification of the high-field electron resonance is possible by performing measurements in Voigt geometry (optical propagation perpendicular to B). If it is due to 2D-like interface carriers, the intensity of the resonance absorption should be strongly reduced in the Voigt geometry.

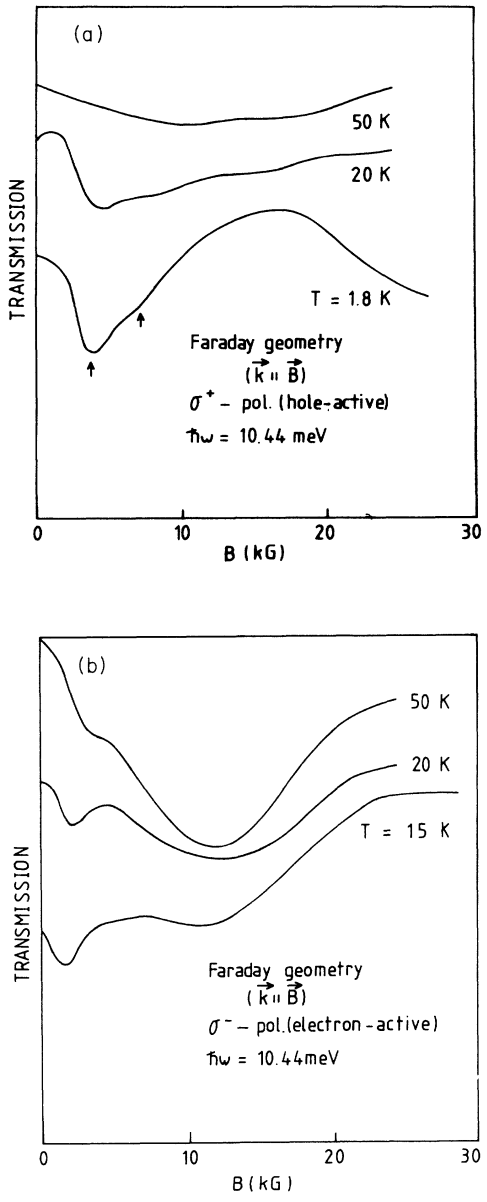

FIG. 4. (a) Temperature dependences of hole cyclotron resonance for a far-infrared energy $\hbar\omega = 10.44$ meV in Faraday geometry (hole-active polarization). (b) Temperature dependences of electron cyclotron resonance for a far-infrared energy $\hbar\omega = 10.44$ meV in Faraday geometry (electron-active polarization).

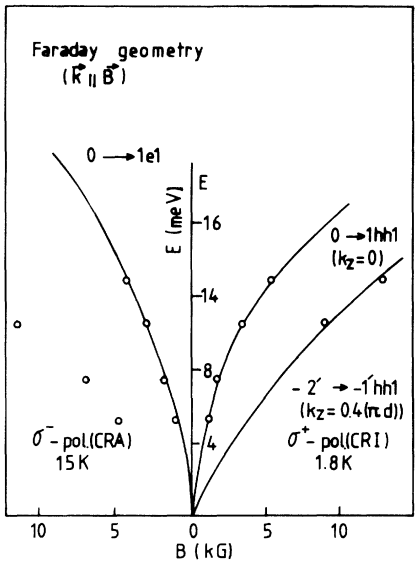

FIG. 5. Far-infrared photon energies as a function of resonant magnetic fields in the Faraday geometry. The solid lines along data are a fit to the calculated inter-Landau-level transitions.

IV. SUPERLATTICE BAND STRUCTURE AND IDENTIFICATION OF INTER-LANDAU-LEVEL MAGNETO-OPTICAL TRANSITIONS

We have calculated the energy band structure in order to identify the magneto-optical intraband transitions and explain the existence of two holes with different mobilities at low temperature as well as the abrupt decrease in their mobilities with increasing temperature. In calculating the band structure by a $\mathbf{k}\cdot\mathbf{p}$ method, the best fit to the experimental data was obtained following slight adjustments of the Zn composition x and layer thicknesses. The value of the valence-band offset Λ ($\simeq 500$ meV), which cannot be uniquely determined by the cyclotron-resonance data in Faraday geometry alone,[8-10] was independently determined by the reflectivity data, as discussed below.

Figure 6 displays the resulting band structure of the su-

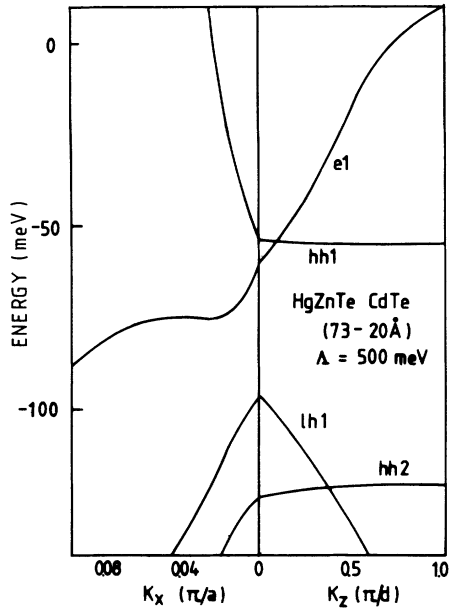

FIG. 6. Calculated superlattice energy dispersions in the growth and in-plane directions.

perlattice for $x=0.04$, $d_W=73$ Å, and $d_B=20$ Å, and the magnetic field dependence of the Landau levels at $k_z=0$ is illustrated in Fig. 7. As seen in Fig. 6, the superlattice is semimetallic, with a negative band gap of 5.75 meV at the zone center. This band structure shows that in contrast to the E1 band, the HH1 band is dispersionless, where hh denotes heavy hole, in the growth direction wave vector k_z, which results in the mass broadening

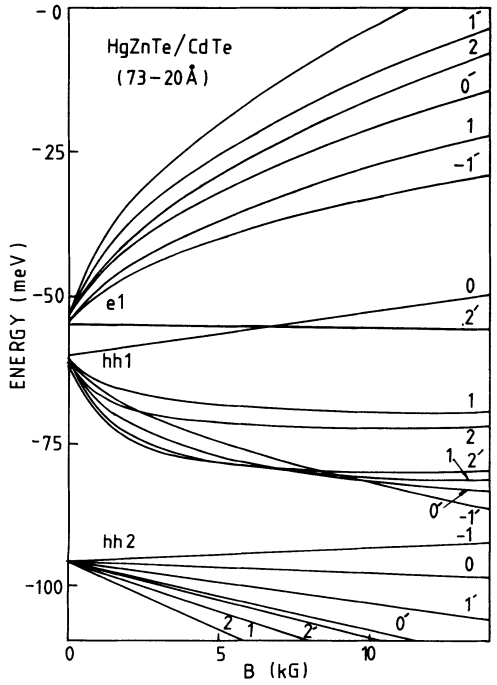

FIG. 7. Magentic field dependence of hole and electron Landau levels at the zone center $k_z=0$.

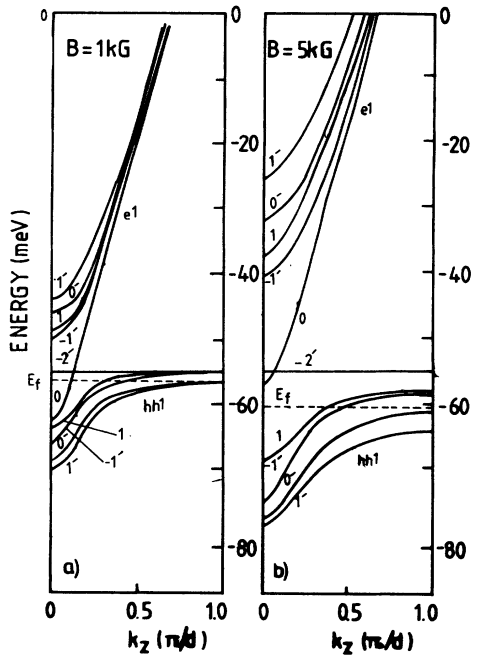

FIG. 8. Energy dispersion of several Landau levels in k_z for $B=1$ kG (a) and for $B=5$ kG (b).

of holes for low temperatures.[5] The hole mass broadening effect on inter-Landua-level transitions can be well understood by energy dispersions of several lowest Landau levels in k_z for a fixed magnetic field, as seen in Fig. 8. The lower hole resonance is found to be very close to the inter-Landau-level transition, $0\Longrightarrow 1\text{hh}1$ (hole active), occurring at $k_z=0$, while the high-field resonance can be fit by the transition, $-2'\Longrightarrow -1'\text{hh}1$, occurring at $k_z\simeq 0.4(\pi/d)$. The reason for the high-field hole resonance to occur at the nonextremal portion of the zone can be explained by considering the position of Fermi level. The Fermi level at nearly zero magnetic field lies about 3 meV below the $-2'$ level, and crosses several hole Landau levels which are condensed together near the zone boundary, as seen in Fig. 8(a). As magnetic field increases, the hole Landau levels are separated from each other and move down far below the $-2'$ level. The Fermi level thus shifts down with increasing magnetic field and crosses the $-1'$ hole Landau level at a nonextremal portion of the zone [Fig. 8(b)]. Therefore, hole states of the $-1'$ level near the extremal portion of the zone boundary are always filled for any magnetic fields, and this prohibits the possible hole transition of $-2'\Longrightarrow -1'\text{hh}1$ near the zone boundary. The hh1 band also shows a strong nonparabolicity of the dispersion with in-plane wave vector k_x, and the average effective mass over the thermal distribution increases with temperature. This causes the abrupt decrease in the hole mobility observed with increasing temperature. This thermal effect in the hole effective mass also accounts for the temperature dependence of the hole cyclotron resonance, which is observed for the wavelength 118.8 μm. As the temperature increases from 1.8 to 50 K, the hole resonances become broader, and another very broad absorp-

tion associated with low mobility holes starts to occur at the high-field side [Fig. 4(a)].

V. REFLECTIVITY AND INTERSUBBAND OPTICAL TRANSITIONS

The existence of holes and their thermal properties should be confirmed as a direct measurement of hole intersubband transitions. This was done in our reflectivity experiment, which is also found to be crucial in determining the Λ. Figure 9 displays the high-frequency reflectivity data of the superlattice. No appreciable structure was found beyond 900 up to 3000 cm^{-1}. In the polarization mode of $E\|z$, the data show a strong absorption at about 570 cm^{-1} and a weak one at about 350 cm^{-1}. The main absorption at 570 cm^{-1} shows a marked polarization dependence, and corresponds to the hh1 $\Longrightarrow$ hh2 intersubband transition. On the other hand, the small absorption at 350 cm^{-1} has relatively little polarization dependence, and is associated with the hh1 $\Longrightarrow$ lh1 transition (the polarization selection rule is less restrictive for interband transitions than intersubband transitions). Both absorptions also have temperature-induced broadenings, as shown in Fig. 10. We note that with increasing temperature, the hh1 $\Longrightarrow$ hh2 absorption becomes weaker and its transition energy is found to shift to lower energy. This thermal behavior was first thought to arise from the temperature dependence of the band gap, however, the calculation shows that if we consider the temperature dependence only through the band gap in $Hg_{1-x}Zn_xTe$ wells while the valence-band offset is assumed to be constant, then the heavy-hole subband edge positions do not change. When the temperature is increased highly enough above 100 K, the superlattice becomes semiconducting with a positive band gap, while the unique nonparabolic and anisotropic feature of the valence band is still alive (this is quite different from the behavior of the conduction band which becomes nearly isotropic in semiconducting regime). The thermal shift of absorption position in the

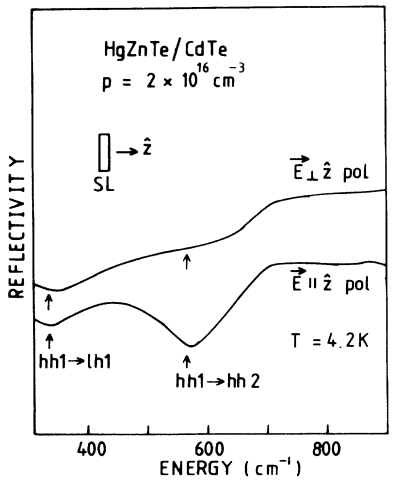

FIG. 9. Polarization dependence of reflectivity spectra at 4.2 K.

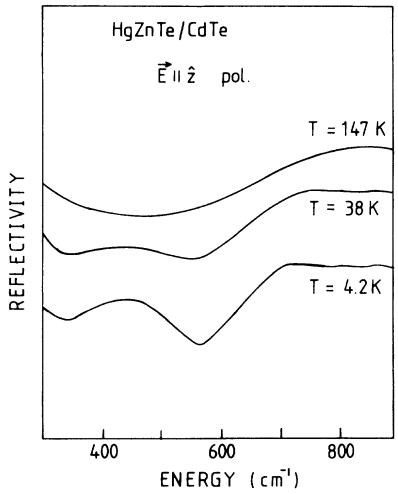

FIG. 10. Temperature dependence of reflectivity for polarization perpendicular to the superlattice plane.

reflectivity can thus be explained by the strong nonparabolicity of the hh1 in-plane energy dispersion $E(k_x)$, similar to those in the transport and the hole cyclotron-resonance data. As temperature increases, thermally excited holes are distributed over the high-energy region of the hh1 band, resulting in the small shift of hh1 $\Longrightarrow$ hh2 transition to lower energy.

The observed transition energy of hh1 $\Longrightarrow$ hh2 is found to fall at about 70 meV. This result is crucial in determining the value of Λ. It is well known that strain moves the light-hole band lh1 higher in energy with respect to hh1, while quantum confinement enhanced by a large Λ pushes lh1 lower than hh1 because of the large difference between light-hole and heavy-hole masses.[11] Therefore, for small Λ values the strain effect is dominant, and the hole Fermi level is on the lh1. The intersubband transition is then lh1 $\Longrightarrow$ lh2 whole transition energy is very large ($\simeq$200 meV) because of the small light-hole mass. Thus, the observed transition energy of about 570 cm^{-1} cannot be explained by any optical transitions between light-hole subbands. The assignment of the main absorption of 570 cm^{-1} to the hh1 $\Longrightarrow$ hh2 intersubband transition implies that the Fermi level is in the hh1 band, and this is possible only for large values of the valence-band offset. The theoretical value of Λ for fit to the reflectivity data should be determined so as to be consistent with the transport and magneto-optical data. For $x=0.04$, $d_w=73$ Å and $d_B=20$ Å, the value of $\Lambda=500$ meV gives $E(\text{hh1}\Longrightarrow\text{hh2})=70$ meV, $E(\text{hh1}\Longrightarrow\text{lh1})=45$ meV, and the negative band gap $E_g=-5.75$ meV. The values of deformation potentials for the strain are taken identical to those in HgTe,[10] and their small dependence on x has been neglected, which may be justified for $Hg_{1-x}Zn_xTe$ with low Zn content.

VI. CONCLUSION

The transport and magneto-optical measurements done on the p-type $Hg_{1-x}Zn_xTe$/CdTe suprelattice show consistent behavior of two holes with different mobilities,

which is explained by the extremely nonparabolic and anisotropic valence-band structure. Properties of the holes were further investigated by reflectivity measurements, which led to identification of the two transitions, hh1 $\Longrightarrow$ hh2 and hh1 $\Longrightarrow$ lh1. The main absorption of the hh1 $\Longrightarrow$ hh2 at 570 cm^{-1} shows a strong polarization dependence and a temperature-induced broadening and shift in transition energy. Considering the compensating effect of the quantum confinement and strain on the position of hole subbands, this result also gives direct experimental evidence for a large value ($\simeq$500 meV) of the valence-band offset. However, it should be noted that there are enough uncertainties in the Zn composition x and the layer thicknesses of the superlattice that slightly smaller values of the offset cannot be ruled out.

ACKNOWLEDGMENTS

One of the authors (J.B.C.) would like to acknowledge partial support of this work by the Korea Science and Engineering Foundation through the Korea-United States International Cooperative Research Program, the Korea Research Foundation, and the Agency for Defense Development in Korea.

*Permanent address: Department of Physics, Kyung Hee University, Seoul 130-701, Korea.

†Permanent address: Department of Physics, Sejong University, Seoul 133-747, Korea.

‡Permanent address: Department of Physics, Dongguk University, Seoul 100-715, Korea.

[1]J. R. Meyer, R. J. Wagner, F. J. Bartoli, C. A. Hoffman, M. Dobrowolska, T. Wojtowicz, J. K. Furdyna, and L. R. Ram-Mohan, Phys. Rev. B **42**, 9050 (1990).

[2]J. R. Meyer, C. A. Hoffman, F. J. Bartoli, T. Wojtowicz, M. Dobrowolska, J. K. Furdyna, X. Chu, J. P. Faurie, and L. R. Ram-Mohan, Phys. Rev. B **44**, 3455 (1991).

[3]J. R. Meyer, D. J. Arnold, C. A. Hoffman, F. J. Bartoli, and L. R. Ram-Mohan, Phys. Rev. B **46**, 4139 (1992).

[4]J. R. Meyer, C. A. Hoffman, F. J. Bartoli, J. W. Han, J. W. Cook, Jr., J. F. Schetzina, X. Chu, J. P. Faurie, and J. N. Schulman, Phys. Rev. B **38**, 2204 (1988).

[5]C. A. Hoffman, J. R. Meyer, F. J. Bartoli, J. W. Han, J. W. Cook, J. F. Schetzina, and J. N. Schulman, Phys. Rev. B **39**, 5208 (1989).

[6]J. M. Berroir, Y. Guldner, J. P. Vieren, M. Voos, X. Chu, and J. P. Faurie, Phys. Rev. Lett. **62**, 2024 (1989).

[7]J. Manasses, Y. Guldner, J. P. Vieren, M. Voos, and J. P. Faurie, Phys. Rev. B **44**, 13 541 (1991).

[8]J. M. Berroir, Y. Guldner, J. P. Vieren, M. Voos, and J. P. Faurie, Phys. Rev. B **34**, 891 (1986).

[9]N. F. Johnson, P. M. Hui, and H. Ehrenreich, Phys. Rev. Lett. **61**, 1933 (1988).

[10]J. B. Choi, L. Ghenim, R. Mani, H. D. Drew, K. H. Yoo, and J. T. Cheung, Phys. Rev. B **41**, 10 872 (1990).

[11]J. R. Meyer, F. J. Bartoli, C. A. Hoffman, and J. N. Schulman, Phys. Rev. B **38**, 12 457 (1988).